



NOVA R & D Inc.

1525 Third St., Suite C
Riverside, CA 92507, USA
www.novarad.com

Tel: 909.781.7332
Fax: 909.781.0178
nova@novarad.com

Development of low power high speed readout electronics for high resolution PET with LSO
and APD arrays

Gerard Visser, Simon Cherry, Martin Clajus, Yiping Shao, and Tümay O. Tümer

This work has been submitted to the IEEE for publication. Copyright may be transferred without notice, after which this version may no longer be accessible

Development of low power high speed readout electronics for high resolution PET with LSO and APD arrays

Gerard Visser, Simon Cherry, Martin Clajus, Yiping Shao, and Tümay O. Tümer

Abstract—An ASIC-based readout electronics scheme is under development for high resolution, compact PET imagers based on independent readout of all channels of LSO scintillator and avalanche photodiode (APD) arrays. Depth of interaction is obtained by readout of both ends of the LSO crystals. A low power, highly integrated design is critical. We report here on a discrete electronics prototype, running at 22 mW per channel for the preamplifier and discriminator. The measured timing resolution is 3.6 ns FWHM, 9.2 ns full width at one tenth maximum, relative to an LSO/PMT detector, energy resolution is 13.3 % FWHM at 511 keV, and depth of interaction position resolution is 2.5 mm FWHM throughout the full length of the crystal. Work is in progress towards an ASIC and a full scale prototype detector module suitable for a high resolution compact PET instrument.

I. INTRODUCTION

THERE has been considerable interest in recent years in developing dedicated high resolution positron emission tomography (PET) systems for applications in breast cancer imaging [1]-[7] and small-animal imaging [8]-[13]. The goal in these systems is to achieve much higher spatial resolution and sensitivity for specific tasks than is possible with whole-body PET scanners designed for general purpose use. A second goal is to produce relatively inexpensive, compact and easy to use systems that make PET more accessible. Generally, these dedicated systems use small scintillator elements read out by position-sensitive or multi-channel PMTs. In most systems, some form of signal multiplexing is used to reduce the number of channels to a manageable number. Since the predominant mode of interaction at 511 keV in all scintillators currently used for PET is Compton scatter, multiplexing can lead to significant loss of position information. Furthermore, depth of interaction (DOI) blurring

becomes a prominent feature in these small diameter systems, and therefore several groups have been exploring detector approaches that can measure DOI [14]-[16].

Recently, avalanche photodiode (APD) arrays have become available that when combined with Lu_2SiO_5 (LSO) scintillator crystals offer new opportunities for high resolution PET detectors [14],[17]-[20]. This work focuses on the high-gain APD arrays developed by RMD, Inc. (Watertown, MA) [17]. The APD arrays are available with a 2.48 mm (16 channels) or a 1.27 mm pitch (64 channels); the 2.48 mm pitch array which we work with here has a pixel active area of $2 \text{ mm} \times 2 \text{ mm}$, a gain of order 1000, and capacitance per pixel of 2.8 pF [21]. For room temperature operation, the leakage current is around 100 nA and the current noise is around $5 \text{ pA}/\sqrt{\text{Hz}}$, when operated near maximum gain (for optimal timing resolution). The quantum efficiency is greater than 60 % at 420 nm, the peak emission wavelength of LSO. The work reported here has been performed with a single channel APD of the same $2 \text{ mm} \times 2 \text{ mm}$ geometry and the same specifications.

The compact geometry and low mass of the APD arrays allow for double-ended readout of the LSO crystals, to make DOI measurements, with the added engineering advantage of identical readout electronics for both sides of the crystal array. DOI measurement is critical to achieving uniformly high spatial resolution in combination with high sensitivity in an affordable instrument, with a ring diameter of about 20 cm. Furthermore, the use of completely independent readout channels for each crystal of the array, instead of a position sensitive readout scheme, may enable the accurate analysis, or the unambiguous rejection, of some events involving Compton interactions in the scintillator array. Overall system deadline can also be significantly reduced by using independent readout channels for each crystal of the array.

Individual readout of each crystal of the array places a high premium on cost, power dissipation, and size and mass of the readout electronics. Most readout functions, including all functions required on a per-channel basis, will have to be integrated into an ASIC before such a system becomes viable. A complete, highly integrated, low power readout ASIC optimized for high resolution PET imaging with LSO/APD arrays is to date not available, although encouraging results have been reported for individual circuit blocks such as the

This work was supported in part by the U.S. Department of Energy under Grant No. DE-FG03ER83058.

Gerard Visser, Martin Clajus, and Tümay Tümer are with NOVA R & D, Inc., Riverside CA 92507 USA (telephone: 909-781-7332, e-mail: gerard.visser@novarad.com).

Simon Cherry is with the Department of Biomedical Engineering, University of California at Davis, Davis CA 95616 USA (telephone: 530-754-9419, e-mail: srcherry@ucdavis.edu)

Yiping Shao was with the Crump Institute for Molecular Imaging, Department of Molecular and Medical Pharmacology, University of California at Los Angeles. He is now with GE Corporate R & D, Niskayuna, NY 12309 USA (telephone: 518-387-6433, e-mail: shao@crd.ge.com).

preamplifier and discriminator [22], [23]. We are working to develop such readout electronics, specifically optimized to meet the crystal identification, timing, energy, and DOI requirements of high resolution PET while minimizing system complexity and cost. In this paper we present results from a discrete electronics prototype, confirming that the architecture and specifications of our readout electronics will deliver the performance required for high resolution PET. We are currently working towards an ASIC-based prototype LSO/APD array module.

II. THE PROTOTYPE SYSTEM

The APD gain is sufficiently high that the principal electronics noise contribution in the system is the current noise of the APD itself. Therefore we use a transimpedance amplifier input stage instead of a charge sensitive amplifier. The design minimizes power while preserving the relatively short (5 to 10 ns) risetime of the LSO/APD signal. Since the APD capacitance is only about 2.8 pF, the transimpedance amplifier can have a wide bandwidth with still relatively small noise contributions from the voltage noise of the open loop amplifier and the current noise of the feedback resistor.

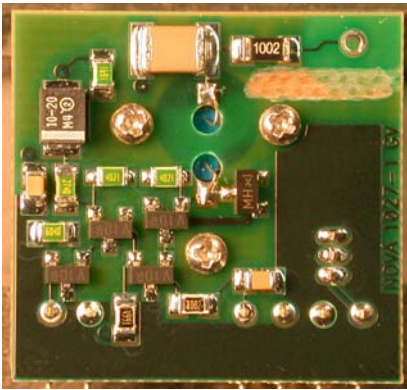


Fig. 1. Prototype APD / transimpedance amplifier module. The APD is mounted in a Delrin block on the back side of the board, and wired through the holes seen near the middle of this photo. This assembly attaches (by means of the three #0-80 screws) to another Delrin block holding the LSO crystal. An identical APD assembly is on the other end of the LSO crystal.

A photo of the transimpedance amplifier input stage mounted together with the APD is shown in Fig. 1. This stage is followed by a second gain stage with differential output; the overall transimpedance is 43.4 k Ω to the differential output. The bandwidth (calculated from response to an input pulse step) is 77 MHz. Fig. 2 shows the noise voltage spectrum out of the amplifier with and without the contribution of the APD current noise. We have not yet had the opportunity to optimize the system performance (especially timing resolution) by selecting the amplifier bandwidth, but we do plan to explore this. Excess bandwidth (beyond what is required to faithfully follow the LSO/APD output pulses) will be detrimental because of the added noise.

For the timing pick-off, a leading edge discriminator is used. This will lead to time walk, although – since the system noise is low enough to allow a threshold around 50 keV or

less – the time walk for energies relevant to PET is under control. The long crystals, with surfaces optimized for DOI measurement, add the complication that the pulse height, even for the photopeak, may be small for one of the APDs; to cope with this, we take the time pick-off from either the front or back APD, whichever is the first to cross threshold.

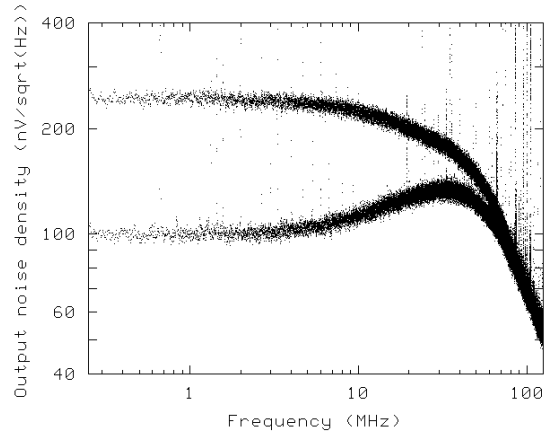


Fig. 2. Transimpedance amplifier output noise spectral density, with and without contribution of APD current noise (APD bias 1755 V and 1600 V; at 1600 V the gain is greatly reduced but the capacitance is essentially the same). The spikes are artifacts of the oscilloscope FFT.

For the pulse height measurement we use a two-pole low pass filter to shape the pulses with a peaking time of 180 ns, and capture the pulse height in a sample and hold circuit timed from the discriminator output. The pulse height is then digitized by a 12-bit successive-approximation A/D converter. (The ASIC will also include a sparse readout circuit to read the pulse height from the front and back APDs of all and only those LSO crystals which are over threshold for a given event.)

III. RESULTS

The prototype system was studied for depth of interaction, energy, and timing resolution. For all of these measurements the APD bias voltages were 1752.3 V and 1737.3 V, with absolute accuracy $\pm 1.5\%$; stability and peak-to-peak noise is less than 100 mV. The bias voltages were tuned for the maximum reasonable gain, beyond which the preamplifier output showed a significantly increased noise level. The average photopeak pulse amplitudes seen from the two APDs were within a factor of two of one another. The measured temperature was 30 $^{\circ}\text{C}$, but no active temperature control system was used.

The discriminator thresholds were set at 177 nA and 99 nA, respectively. Pulses from the 511 keV photopeak signal have an amplitude around 1.9 μA , by comparison, so that in energy terms the timing threshold is set less than 47 keV.

The LSO crystal dimensions were 2 mm \times 2 mm \times 20 mm; the long faces were plain saw-cut surfaces and both 2 mm \times 2 mm end faces were mechanically polished. The crystal was wrapped in white teflon tape and coupled to the APDs with a small amount of Bicorn BC-630 optical grease.

The second detector for all our measurements was composed of a polished $2\text{ mm} \times 2\text{ mm} \times 10\text{ mm}$ LSO crystal, coupled end-on to a Hamamatsu R1635 PMT. A leading edge discriminator (constructed from a Motorola MC100LVEL16 integrated circuit) was used for timing from the PMT.

A. Depth of Interaction

For the DOI tests, a $3.21\text{ MBq }^{22}\text{Na}$ source (diameter 1 mm) was placed at a distance of 48 mm perpendicularly from the side of the LSO crystal. The LSO/PMT detector was placed at a distance of 72 mm on the far side of the source. Thus in coincidence a spot size of order of 1.4 mm FWHM is illuminated on the $2\text{ mm} \times 2\text{ mm} \times 20\text{ mm}$ LSO crystal, ignoring the effects of the positron range and momentum. The PMT and the source are fixed to a linear motion table parallel to the $2\text{ mm} \times 2\text{ mm} \times 20\text{ mm}$ LSO crystal. The position of the motion table, and hence of the illuminated spot on the LSO crystal, is labeled here by the coordinate ‘ z ’. No absolute position calibration was used; $z = 0\text{ mm}$ is arbitrary, though it is near the back end of the crystal. We recorded 5000 events at each z position from $z = 0\text{ mm}$ to 21 mm by steps of 1 mm .

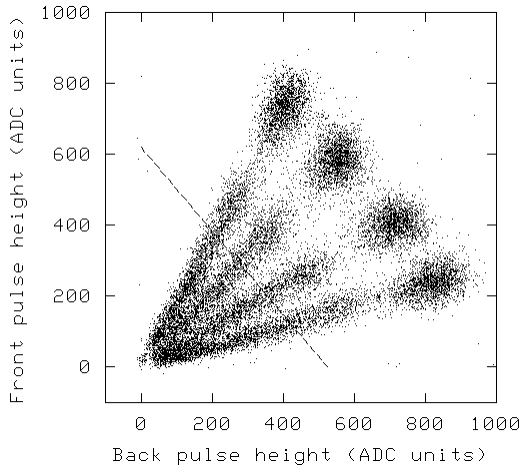


Fig. 3. Front vs. back pulse height scatter plot, aggregate of four different z positions (1 mm , 7 mm , 13 mm , 19 mm). The dashed line shows the location of an approximate energy cut at 250 keV used in some of the analysis ($F/620 + B/525 > 1$).

DOI measurement proceeds by a comparison of the scintillation light detected at the front and back ends of the crystal. Fig. 3 shows a scatter plot of pulse height measured on the front APD (F) vs. pulse height measured on the back APD (B), with the source located successively at four different z positions separated by 6 mm . The energy and DOI capability can be quickly appreciated from a consideration of this plot. The baseline level digitized from the A/D converter with zero pulse input has been subtracted from this data (and similarly for the remainder of this paper). No other corrections have been applied to the pulse height data as measured by the A/D converter.

For events at a given z position, the ratio of the front APD pulse height to back APD pulse height is expected to be a constant, and ideally there is a one-to-one correspondence between z and the ratio F/B . It is convenient to use the ratio

$F/(F+B)$, or the angle $\arctan(F/B)$, for analysis instead of the ratio F/B . Fig. 4 shows histograms of the angle determined from the front to back pulse height ratio.

DOI resolution is degraded for low-energy events, where the angular separation in the front vs. back scatter plot evidently is not as great. Typically, however, lower energy thresholds of between 250 and 350 keV are used in a PET system. We therefore also explore the effect of an energy cut (shown by the dashed line in Fig. 3) on the DOI resolution.

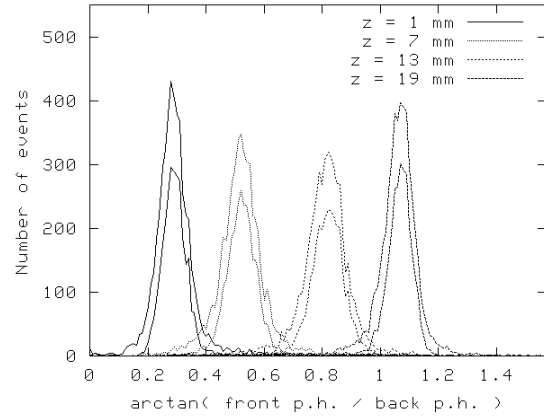


Fig. 4. Histograms of the angle determined by front to back pulse height ratio for the same data shown in Fig. 3. These histograms are shown with and without the energy cut at approximately 250 keV .

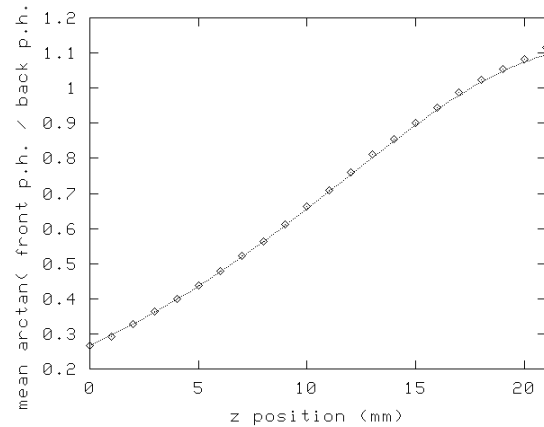


Fig. 5. Measured relationship of z position to pulse height ratio, with a polynomial fit.

The position of the event may be inferred from the measured front to back pulse height ratio. From our data we obtain the calibration curve shown in Fig. 5. The position resolution is shown in Fig. 6. Over the central 16 mm of the crystal, the position resolution averages 2.86 mm FWHM if no energy cut is applied, and 2.53 mm FWHM when the energy cut is used. The position resolution degrades at the ends of the crystal, probably due to the effects of direct interactions in the APDs and to the fact that this data is taken at a constant number of events for each z position, obviously increasing the relative contribution of Compton scattered events when the main photon beam is past the end of the crystal. However, if the physical constraint that the interaction occurs inside the crystal is taken into account, then measured position FWHM around 2.5 mm can be recovered.

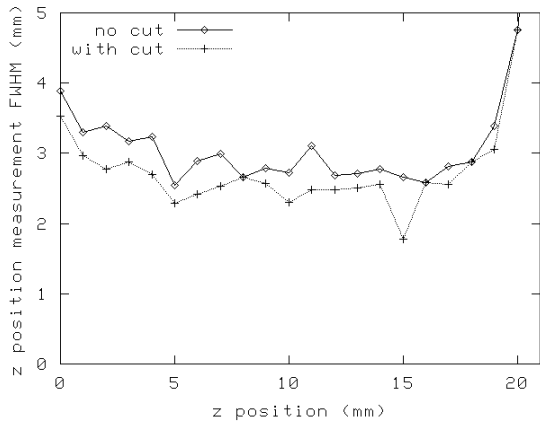


Fig. 6. DOI position resolution, with and without the cut at approximately 250 keV. At $z = 20$ mm the end of the crystal is hit, and the apparent DOI resolution degrades considerably.

B. Energy

To discuss the energy resolution, it is again useful to start with an examination of the front vs. back pulse height scatter plot. With the same data set above, Fig. 7 shows the front vs. back pulse height in aggregate for all z positions. (Note that the distribution of events in z is roughly uniform, which will not normally be the case in PET, of course.)

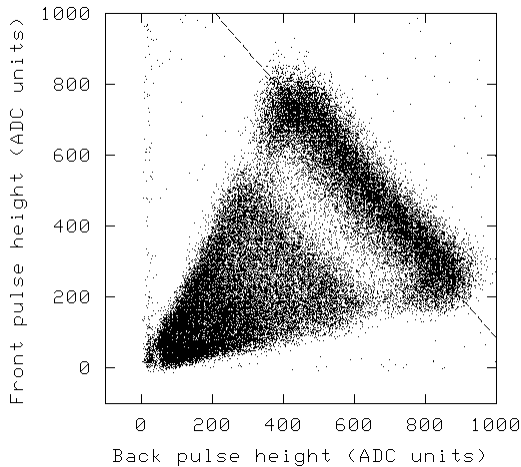


Fig. 7. Front vs. back pulse height scatter plot, aggregate of all z positions. The dashed line is a linear fit to the photopeak region.

As a first approximation, the energy may be expressed as $E = \alpha F + \beta B$. The relative coefficients are determined by a line fit to the photopeak region in the scatter plot. The resulting energy spectrum is shown in Fig. 8. The energy resolution is 13.3 % FWHM. The observed photopeak to Compton ratio is 0.707, which is roughly in agreement with the 0.521 expected for a small LSO scintillator [24]. The discrepancy probably can be attributed to the nonzero energy threshold and to multiple-interaction events.

In the front-back scatter plot two effects are clearly visible which can limit the energy resolution, at least in principle. The photopeak does not appear as a perfectly straight line, but rather is bowed in slightly in the middle region, indicating, as is to be expected, a lower light collection efficiency for events

near the middle of the crystal. Also the photopeak is broadened and reduced in amplitude near the ends of the crystal, which can probably be attributed to total internal reflection from the end of the crystal. The critical angle between LSO and BC-630 grease is 53.6° , so this only begins to occur within 1.47 mm of the ends.

The depth of interaction information may be applied in an attempt to improve the energy resolution, writing the energy as $E = (\alpha F + \beta B)f(F/B)$ and determining the coefficients and the correction function f from a fit to the photopeak region in the scatter plot. Unfortunately we obtained no significant improvement in the energy resolution, but in some cases there may be hope of a useful improvement.

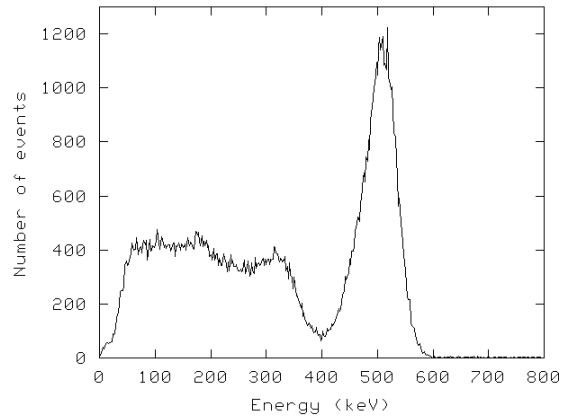


Fig. 8. Measured energy spectrum of 511 keV photons. The resolution is 13.3 % FWHM.

C. Timing

We studied the coincidence time resolution (Fig. 9) with the LSO/APD and LSO/PMT detectors positioned in a line, 140 mm apart, and the source mid-way between them. The time difference was measured using a TDS7104 digital oscilloscope (bandwidth 1 GHz, sample interval 200 ps) in delay measurement mode. With no explicit energy cut the coincidence time resolution is 4.6 ns FWHM. Applying a cut for greater than 250 keV, coincidence time resolution is 3.6 ns FWHM, 9.2 ns full width at one-tenth maximum; time walk correction reduces this to 3.4 ns FWHM, 7.5 ns FWTM.

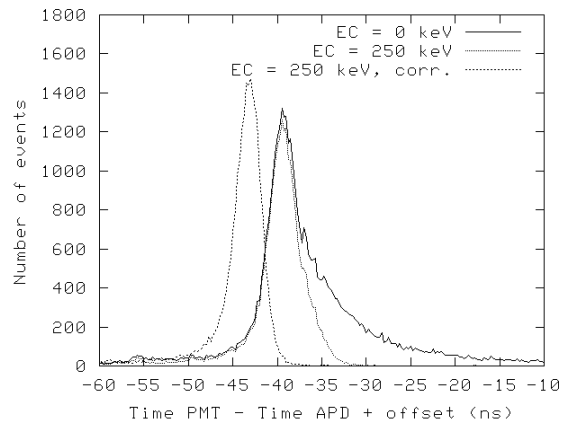


Fig. 9. Coincidence time spectrum, for all events, for events with a 250 keV cut, and with a 250 keV cut and time walk correction applied.

The time walk scatter plot is shown in Fig. 10. Some amount of time walk is evident at all energies, although above 250 keV the effect of time walk is minimal. If required, residual time walk correction could be applied by programmable logic resources on the detector module board.

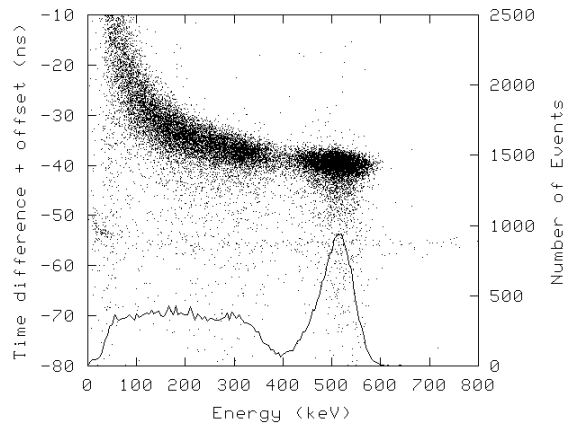


Fig. 10. Time walk scatter plot. Note that events below the main curve show time walk in the LSO/PMT detector, and these errors are therefore not correlated with the energy measured in the LSO/APD detector.

The resolution is limited by time walk in the LSO/PMT readout (left side of the peak in Fig. 9), and possibly by noise in the APD readout electronics. We will address these issues by optimizing the amplifier bandwidth and gain, and by making direct APD/LSO – APD/LSO timing measurements (at present, we have used only a single APD/LSO detector).

IV. CONCLUSIONS

The work described above has demonstrated the potential performance capabilities for a compact, high resolution PET instrument based on LSO scintillator arrays with double-ended readout by APD arrays. The depth-of-interaction, energy, and timing resolution meet the requirements for high resolution PET, although it must be considered that performance with a scintillator array will be somewhat worse, owing to the effects of optical and possibly electronic crosstalk and of Compton scattering between crystal elements. Our next stage will be to design and fabricate an ASIC to implement the readout functions currently done with the discrete electronics we described, and to instrument an LSO crystal array with this ASIC and verify the performance under these more realistic conditions. Since the DOI resolution shown here is relatively good, there will probably be sufficient margin to increase the crystal length beyond 20 mm, which will boost the detection efficiency further.

V. REFERENCES

- [1] R.R. Raylman, S. Majewski, R. Wojcik, A.G. Weisenberger, B. Kross, V. Popov, H. Bishop. "The potential role of positron emission mammography for detection of breast cancer. A phantom study." *Med Physics* **27** 1943 (2000).
- [2] C. J. Thompson, K. Murthy, Y. Picard, et al., "Positron Emission Mammography (PEM): A Promising Technique for Detecting Breast Cancer." *IEEE Trans. Nucl. Sci.*, **42**, 1012 (1995).
- [3] I. Weinberg et al., "Preliminary Results for Positron Emission Mammography: Real-time Functional Breast Imaging in a

- Conventional Mammography Gantry." *Eur. Journal of Nuclear Medicine*, **23**, 804 (1996).
- [4] R. Freifelder and J. Karp, "Dedicated PET Scanners for Breast Imaging." *Physics in Medicine and Biology*, **42**, 2463 (1997).
- [5] G. Hutchins and A. Simon, "Evaluation of Prototype Geometries for Breast Imaging with PET Radiopharmaceutical." *Journal of Nuclear Medicine*, **36**, 69P (1995).
- [6] W.W. Moses, T.F. Budinger, R.H. Huesman, et al., "PET Camera Designs for Imaging Breast Cancer and Axillary Node Involvement." *Journal of Nuclear Medicine*, **36**, 69P (1995).
- [7] N.K. Doshi, Y. Shao, R.W. Silverman, and S.R. Cherry, "maxPET: A dedicated mammary and axillary region PET imaging system for breast cancer," *IEEE Trans. Nucl. Sci.*, vol. 48, pp. 811-815, 2001
- [8] S. R. Cherry, Y. Shao, R. W. Silverman, K. Meadors, S. Siegel, A. Chatziioannou, et al., "MicroPET: a high resolution PET scanner for imaging small animals," *IEEE Trans. Nucl. Sci.*, vol. 44, pp. 1161-1166, 1997.
- [9] A. P. Jeavons, R. A. Chandler, and C. A. R. Dettmar, "A 3D HIDAC-PET camera with sub-millimetre resolution for imaging small animals," *IEEE Trans. Nucl. Sci.*, vol. 46, pp. 468-473, 1999.
- [10] S. I. Ziegler, B. J. Pichler, G. Boening, M. Rafecas, W. Pimpl, E. Lorenz, et al., "A prototype high-resolution animal positron tomograph with avalanche photodiode arrays and LSO crystals," *European Journal of Nuclear Medicine*, vol. 28, pp. 136-143, 2001.
- [11] S. Weber, H. Herzog, M. Cremer, R. Engels, K. Hamacher, F. Kehren, et al., "Evaluation of the TierPET system," *IEEE Trans. Nucl. Sci.*, vol. 46, pp. 1177-1183, 1999.
- [12] R. Lecomte, J. Cadorette, S. Rodrigue, D. Lapointe, D. Rouleau, M. Bentourkia, et al., "Initial results from the Sherbrooke avalanche photodiode positron tomograph," *IEEE Trans. Nucl. Sci.*, vol. 43, pp. 1952-7, 1996.
- [13] A. Del Guerra, G. Di Domenico, M. Scandola, and G. Zavattini, "High spatial resolution small animal YAP-PET," *Nucl. Instr. Meth. A*, vol. 409, pp. 508-510, 1998.
- [14] Y. Shao et al., "Design studies of a high-resolution PET detector using APD arrays," *IEEE Trans. Nucl. Sci.*, vol. 47, no. 3, pp. 1051-1057, June 2000.
- [15] A. Saoudi, C.M. Pepin, F. Dion, M. Bentourkia, R. Lecomte, M. Andreaco, et al., "Investigation of depth-of-interaction by pulse-shape discrimination in multicrystal detectors read out by Avalanche photodiodes," *IEEE Trans. Nucl. Sci.*, vol. 46, pp. 462-467, June 1999.
- [16] J.S. Huber, W.W. Moses, M.S. Andreaco, and O. Petterson, "An LSO scintillator array for a PET detector module with depth of interaction measurement," *IEEE Trans. Nucl. Sci.*, vol. 48, pp. 684-688, June 2001.
- [17] K.S. Shah, R. Farrell, R.F. Grazioso et al., "Planar processed APDs and APD arrays for scintillation detection," *IEEE MIC conf. record*, Seattle, 1999.
- [18] B. J. Pichler, G. Böning, E. Lorenz, R. Mirzoyan, W. Pimpl, M. Schwaiger, and S. I. Ziegler, "Studies with a prototype high resolution PET scanner based on LSO-APD modules," *IEEE Trans. Nucl. Sci.*, vol. 45, no. 3, pp. 1298-1302, June 1998.
- [19] C. Schmelz, S. M. Bradbury, I. Holl, E. Lorenz, D. Renker, and S. Ziegler, "Feasibility study of an avalanche photodiode readout for high resolution PET with nsec time resolution," *IEEE Trans. Nucl. Sci.*, vol. 42, pp. 1080-1084, Aug. 1995.
- [20] R. Chen, A. Fremout, S. Tavernier, P. Bruydonckx, D. Clément, J.-F. Loude, and C. Morel, "Readout of scintillation light with avalanche photodiodes for positron emission tomography," *Nucl. Inst. and Methods A*, vol. 433, pp. 637-645, 1999.
- [21] RMD, Inc., Watertown, MA, Silicon Avalanche Photodiodes: Specifications [Online]. <http://www.rmdinc.com/production/apd.html>.
- [22] D. M. Binkley, B. S. Puckett, M. E. Casey, R. Lecomte, and A. Saoudi, "A power efficient, low noise, wideband integrated CMOS preamplifier for LSO/APD PET systems," *IEEE Trans. Nucl. Sci.*, vol. 47, no. 3, pp. 810-817, June 2000.
- [23] D.M. Binkley, "Performance of non-delay-line constant fraction discriminator timing circuits." *IEEE Trans. Nucl. Sci.* **41**, 1169 (1994)
- [24] M. J. Berger, J. H. Hubbell, S. M. Seltzer, J. S. Coursey, and D. S. Zucker, "XCOM: Photon Cross Section Database (version 1.2)," <http://physics.nist.gov/xcom> [2001, November 17]. National Institute of Standards and Technology, Gaithersburg, MD.